

## Thermoelectric properties of $\text{CuAlO}_2$

K. Park<sup>a,\*</sup>, K.Y. Ko<sup>a</sup>, W.-S. Seo<sup>b</sup>

<sup>a</sup> Department of Advanced Materials Engineering and Center for Advanced Materials, Sejong University,  
98 Kunja-Dong, Kwangjin-gu, Seoul 143-747, Republic of Korea

<sup>b</sup> Korea Institute of Ceramic Engineering and Technology, Seoul 153-023, Republic of Korea

Available online 24 March 2005

### Abstract

Polycrystalline samples of  $\text{CuAlO}_2$  were prepared by a solid state reaction method. The mixture of  $\text{CuO}$  and  $\text{Al}_2\text{O}_3$  powders was calcined at 1073 K for 2 h. The green compacts were sintered at 1433 or 1473 K for 20 h in air and then furnace cooled. The crystalline structure of the sintered  $\text{CuAlO}_2$  bodies was rhombohedral,  $R\bar{3}m$ , along with a very small amount of  $\text{CuO}$  with a monoclinic structure. It was found that the thermoelectric properties of  $\text{CuAlO}_2$  ceramics were significantly dependent on sintering temperature. The power factor increased with increasing temperature. The values of the power factor measured at 1140 K for the  $\text{CuAlO}_2$  samples sintered at 1433 and 1473 K were  $4.98 \times 10^{-5}$  and  $6.62 \times 10^{-5} \text{ Wm}^{-1} \text{ K}^{-2}$ , respectively.

© 2005 Elsevier Ltd. All rights reserved.

**Keywords:**  $\text{CuAlO}_2$ ; Sintering; Electrical conductivity; Milling; Electron microscopy

### 1. Introduction

Thermoelectric materials with high energy conversion efficiency are strongly required for both electric power generation in terms of waste heat recovery and the refrigeration of electronic devices. Thermoelectric materials, such as  $\text{PbTe}$  and  $\text{Bi}_2\text{Te}_3$ , show the high value of the figure of merit,  $Z = \sigma\alpha^2/\kappa$ , where  $\sigma$ ,  $\alpha$ , and  $\kappa$  are the electrical conductivity, Seebeck coefficient, and thermal conductivity, respectively. However, they are easily decomposed or oxidized at high temperatures in air. Therefore, practical utilization of these materials as a power generator has been limited. Metal oxides have attracted attention as promising thermoelectric materials because of their potential to overcome the above-mentioned problems.

Recently, Terasaki et al.<sup>1</sup> have reported on a new thermoelectric material  $\text{NaCo}_2\text{O}_4$ , which has a high figure of merit ( $8.8 \times 10^{-4} \text{ K}^{-1}$ ) and a large thermopower ( $100 \mu\text{V K}^{-1}$ ) at 300 K. However, its application is limited because of the volatility of sodium above 1073 K. It is thus necessary to

investigate new oxide materials with both high performance and environmental stability at high temperatures. To date, several p-type oxide systems, such as  $(\text{Bi}_2\text{Sr}_2\text{O}_4)_x\text{CoO}_2$ ,  $\text{Ca}_3\text{Co}_4\text{O}_9$ , and  $\text{Ca}_2\text{Co}_2\text{O}_5$ , have been extensively studied.<sup>2–5</sup> The development of new oxide materials is still the most important issue for practical applications of thermoelectric power generation. In this work, we have selected as a candidate material  $\text{CuAlO}_2$  with the delafossite structure. The crystalline structure of  $\text{CuAlO}_2$  had been extensively studied by Ishiguro et al.<sup>6</sup> They proposed that  $\text{Cu}^+$  ions are linearly coordinated by two  $\text{O}^{2-}$  ions to form a O–Cu–O dumbbell unit placed parallel to the c-axis, whereas  $\text{Al}^{3+}$  ions are octahedrally coordinated by six  $\text{O}^{2-}$  ions. O-atoms of O–Cu–O dumbbell link all Cu layers with the  $\text{AlO}_2$  layers.

In general, the fabrication process of thermoelectric materials, especially sintering, significantly affects the microstructure and thus changes the thermoelectric properties. In the present study, the influence of the sintering temperature on the microstructure and thermoelectric properties of polycrystalline  $\text{CuAlO}_2$  was studied. Optimization of the sintering process is necessary because the thermoelectric properties of  $\text{CuAlO}_2$  depend greatly on microstructure, i.e., grain size, grain boundary, bulk density, and grain orientation.

\* Corresponding author. Tel.: +82 2 3408 3777; fax: +82 2 3408 3664.  
E-mail address: [kspark@sejong.ac.kr](mailto:kspark@sejong.ac.kr) (K. Park).

## 2. Experimental

The mixture of high-purity CuO and Al<sub>2</sub>O<sub>3</sub> powders and alcohol was ball-milled for 24 h in a Teflon jar using ZrO<sub>2</sub> as the grinding media. The ball-milled slurries were dried at 353 K in an oven for 12 h. The thermal analysis of powder mixtures was carried out using a differential thermal/thermogravimetric analysis (DT/TGA) (TA Instrument SDT-2960) in the temperature range of 293–1473 K at a heating rate of 10 K min<sup>-1</sup> in air. The mixed powders were calcined in a mullite crucible at 1073 K for 2 h. The calcined powders were ball-milled for 24 h and dried at 353 K in an oven for 12 h. The dried powders were pressed using a hand press at a pressure of 98 MPa to prepare pellets of 5 mm thick and 20 mm diameter. The green compacts were heated at 1433 or 1473 K for 20 h in air and then furnace cooled. The sintered compacts were crushed in an alumina mortar and ball-milled in a planetary mill for 5 h. The resulting powders were pressed into pellets of 5 mm thick and 20 mm diameter and sintered at 1433 or 1473 K for 20 h in air.

The crystalline structure of the as-sintered samples was analyzed with X-ray diffraction (XRD) (Rigaku DMAX-2500/PC) using Cu K $\alpha$  radiation at 40 kV and 100 mA. The microstructure of the as-sintered samples was investigated by using a scanning electron microscope (SEM) (Hitachi S4700). The specimens for electrical measurements were cut out of the sintered bodies in the form of rectangular bars of 2 mm  $\times$  2 mm  $\times$  15 mm with a diamond saw and polished with SiC emery papers. Electrical conductivity was measured by the direct current (dc) four-probe method. For thermopower measurements, a temperature difference in the specimen was generated by passing cool air in a quartz protection tube placed near one end of the specimen. The temperature difference between the two ends in the specimens was controlled to be 3–6 K by varying the flowing rate of air. Thermopower measured as a function of the temperature difference gave a straight line, and the Seebeck coefficient was calculated from its slope. The measurements were carried out at 540–1140 K in air.

## 3. Results and discussion

Fig. 1 shows the results of the DTA and TGA measurements for a mixture of CuO and Al<sub>2</sub>O<sub>3</sub> powders. It is seen that there is an endothermic peak at 1342–1368 K, accompanied with the weight loss, due to the solid-state reactions in the oxides. The crystalline structure of the sintered CuAlO<sub>2</sub> bodies is rhombohedral,  $R\bar{3}m$ ,  $a = 2.8567 \text{ \AA}$  and  $c = 16.943 \text{ \AA}$ ,<sup>7</sup> along with a small amount of CuO with a monoclinic,  $a = 4.653 \text{ \AA}$ ,  $b = 3.410 \text{ \AA}$ , and  $c = 5.108 \text{ \AA}$ .<sup>8</sup> The measured lattice parameters closely agree with those previously reported for this material.<sup>9</sup> The following sequence is regarded as the favorable main reaction for the formation of CuAlO<sub>2</sub>: CuO + Al<sub>2</sub>O<sub>3</sub>  $\rightarrow$  CuAl<sub>2</sub>O<sub>4</sub> and

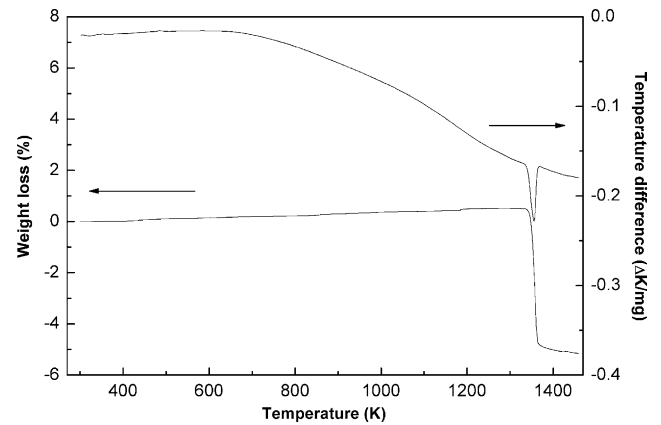


Fig. 1. DTA and TGA results for a mixture of CuO and Al<sub>2</sub>O<sub>3</sub> powders.

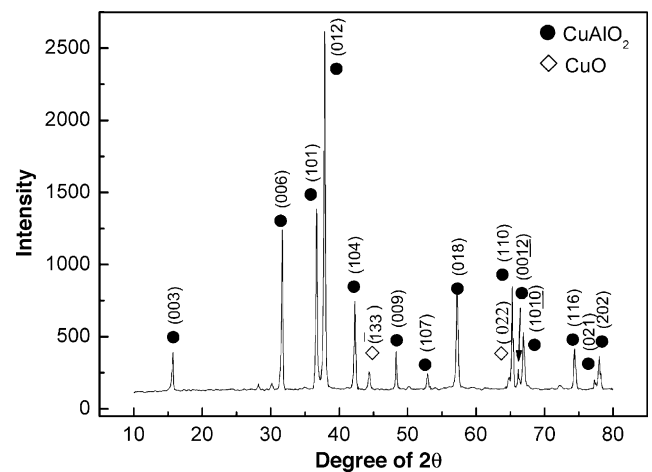


Fig. 2. XRD pattern of the CuAlO<sub>2</sub> sintered at 1473 K.

CuAl<sub>2</sub>O<sub>4</sub> + CuO  $\rightarrow$  2CuAlO<sub>2</sub> + 1/2O<sub>2</sub>. Fig. 2 shows the XRD pattern of the CuAlO<sub>2</sub> sintered at 1473 K.

Fig. 3 shows the SEM image obtained from the surface of the CuAlO<sub>2</sub> sintered at 1473 K. Most pores were located at

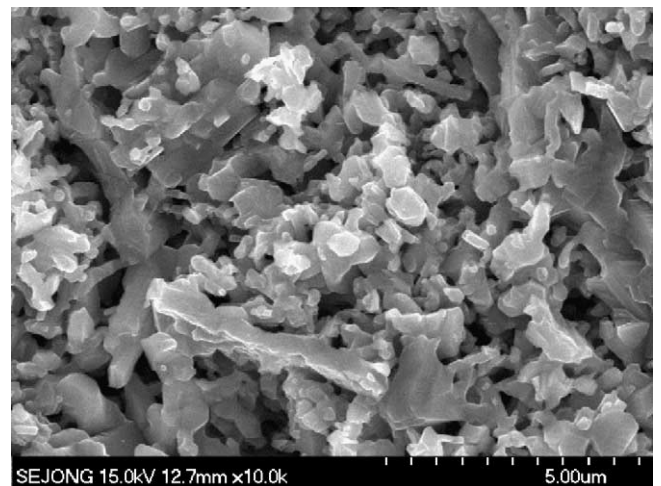


Fig. 3. SEM image obtained from the surface of the CuAlO<sub>2</sub> sintered at 1473 K.

the grain boundaries. It was found that as the sintering temperature increased, the grain size and the density of the samples increased. The bulk density and porosity of the sample sintered at 1433 K are 3.741 g/cm<sup>3</sup> and 26.6%, respectively, while those of the sample sintered at 1473 K are 3.818 g/cm<sup>3</sup> and 25.1%, respectively. The high porosity is responsible for a significant decrease in the electrical conductivity and also the thermal conductivity.<sup>10</sup> It is also important to note that the number of elongated grains and the degree of elongation in elongated grains increased with sintering temperature. The elongated grains may improve the thermoelectric properties.

It was found that the electrical conductivity  $\sigma$  increased with increasing temperature over the measured temperature range, indicating semiconducting behavior, probably because of the deviation from the stoichiometric composition of the components induced by the defect equilibrium.<sup>11</sup> The conductivity of CuAlO<sub>2</sub> sintered at 1473 K is higher than that sintered at 1433 K mainly because of the higher density. The positive holes in CuAlO<sub>2</sub> are generated from ionized Cu vacancies and/or interstitial oxygens within the crystallite sites of the material. The defect chemistry plays an important role in the conductivity. The nonstoichiometric defect reaction for a metal deficient oxide may be represented by the following equation:<sup>11</sup>  $O_2(g) = 2O_O^X + V_{Cu}^- + V_{Al}^{3-} + 4h^+$ , where  $O_O$ ,  $V_{Cu}$ ,  $V_{Al}$  and  $h$  denote lattice oxygen, Cu vacancy, Al vacancy and hole, respectively. Superscripts X, -, and + denote effective neutral, negative and positive charge states, respectively.

Fig. 4 shows  $\ln \sigma$  versus  $1/T$  of the samples from 540 to 1140 K. A linear fit of the data works well in the temperature range of 540–844 K. The linear relation seen in this figure implies a thermally activated hopping conduction, as often found in semiconductors.<sup>12</sup> The conduction takes place via a small-polaron hopping mechanism. From the slope of the graph, we can obtain the value of activation energy  $E_a$

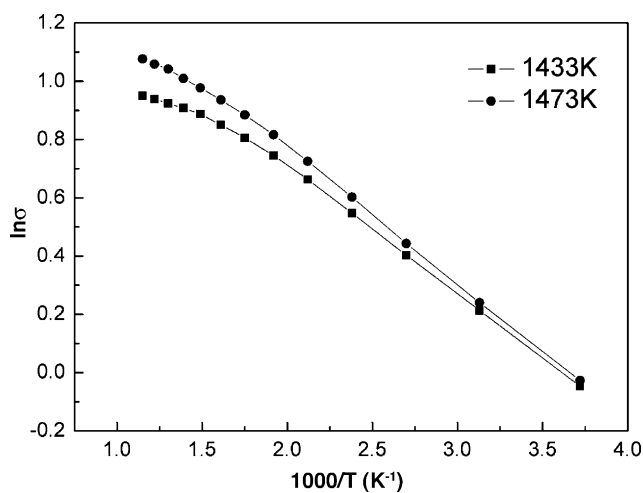


Fig. 4. Relationship between  $\ln \sigma$  and the reciprocal of the absolute temperature ( $1/T$ ) for the CuAlO<sub>2</sub> sintered at 1433 and 1473 K.

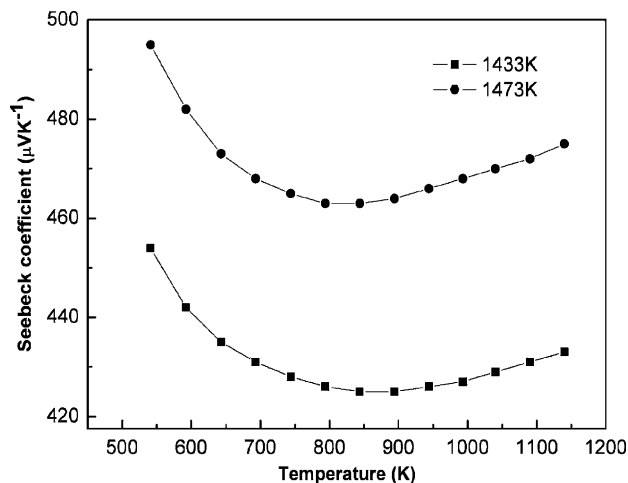


Fig. 5. Seebeck coefficient as a function of temperature for the CuAlO<sub>2</sub> sintered at 1433 and 1473 K.

required to transfer carriers from the acceptor level to the valence band. The value of activation energy is calculated as 0.2 eV, which is smaller than the band gap. The direct and indirect band gaps of CuAlO<sub>2</sub> without any intentional doping are 3.5 and 1.85 eV, respectively.<sup>13,14</sup> Yanagi et al.<sup>15</sup> reported that the calculated activation energy of the CuAlO<sub>2</sub> thin films prepared by the pulsed laser deposition technique is 0.22 eV. To elucidate the detailed nature of the conduction mechanism, further investigation will be necessary, i.e., exact carrier concentrations, the Hall mobility, the spin-state of the electrons, the activation energy of carrier generation and hopping, and the defect structure of the samples.

Fig. 5 shows the Seebeck coefficient  $\alpha$  of the as-sintered CuAlO<sub>2</sub>. The sign of the Seebeck coefficient is positive for the entire measured temperature range, indicating hole conduction.<sup>1–5</sup> The values of the Seebeck coefficient for the CuAlO<sub>2</sub> samples sintered at 1433 and 1473 K decreased up to 844 and 794 K, respectively, because of an increase in the carrier concentration and then increased because of a decrease in the carrier concentration.<sup>16</sup> The relationship between the Seebeck coefficient  $\alpha$  and the carrier concentration  $n_c$  can be expressed as follows:<sup>16</sup>  $\alpha \approx r - \ln n_c$ , where  $r$  is the scattering factor. The positive temperature dependence of the Seebeck coefficient is thought to be due to hopping conduction.<sup>5</sup> It has been previously reported that the Seebeck coefficients for Ca<sub>3</sub>Co<sub>4</sub>O<sub>9</sub> and Ca-doped RCoO<sub>3</sub> (R = Gd, Sm, Nd, and Pr) monotonically increased and decreased, respectively, with an increase in temperature.<sup>3,17</sup>

The power factor  $\sigma\alpha^2$  evaluates the thermoelectric performance of electrical components. The temperature dependence of the power factor calculated from the data in Figs. 4 and 5 is plotted in Fig. 6. The power factor increases up to 1140 K. The values of the power factor measured at 1140 K for the CuAlO<sub>2</sub> samples sintered at 1433 and 1473 K are  $4.98 \times 10^{-5}$  and  $6.62 \times 10^{-5}$  Wm<sup>-1</sup> K<sup>-2</sup>, respectively. To improve the power factor, it is required to optimize

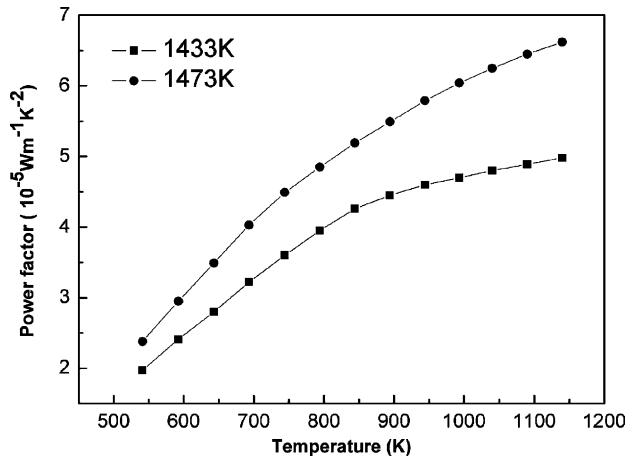


Fig. 6. Temperature dependence of the power factor for the CuAlO<sub>2</sub> sintered at 1433 and 1473 K.

the fabrication process and to incorporate the dopants into CuAlO<sub>2</sub>. The dopant addition increases both the electrical conductivity and the Seebeck coefficient. For example, the addition of a small amount of Pb to Bi<sub>2.3</sub>Sr<sub>2.6</sub>Co<sub>2</sub>O<sub>y</sub> led to an increase in the electrical conductivity and the Seebeck coefficient, which improved the power factor by 3–4 times.<sup>4</sup>

#### 4. Conclusions

XRD patterns showed that the crystalline structure of the sintered CuAlO<sub>2</sub> bodies was identified as rhombohedral, *R*3̄*m*, along with a small amount of CuO with a monoclinic structure. It was found that the higher the sintering temperature, the larger the grain size of the samples and the higher the degree of elongation in elongated grains. The electrical conductivity increased with increasing temperature in the temperature range of 540–1140 K, indicating semiconducting behavior. This is probably due to the deviation from the stoichiometric composition of the components. The values of the Seebeck coefficient for the CuAlO<sub>2</sub> samples sintered at 1433 and 1473 K decreased up to 844 and 794 K, respectively, and then increased. The power factor increased with temperature, and the highest value of power factor for the CuAlO<sub>2</sub> sintered at 1473 K was  $6.62 \times 10^{-5} \text{ Wm}^{-1} \text{ K}^{-2}$ .

#### Acknowledgement

The authors would like to acknowledge the financial support provided for this research by the Korea Energy Management Corporation (KEMCO).

#### References

1. Terasaki, I., Sasago, Y. and Uchinokura, K., Large thermoelectric power in NaCo<sub>2</sub>O<sub>4</sub> single crystals. *Phys. Rev.*, 1997, **B56**, R12685–R12687.
2. Funahashi, R. and Matsubara, I., Thermoelectric properties of Pb- and Ca-doped (Bi<sub>2</sub>Sr<sub>2</sub>O<sub>4</sub>)<sub>x</sub>CoO<sub>2</sub> whiskers. *Appl. Phys. Lett.*, 2001, **79**, 362–364.
3. Masuda, Y., Nagahama, D., Itahara, H., Tani, T., Seo, W. S. and Koumoto, K., Thermoelectric performance of Bi- and Na-substituted Ca<sub>3</sub>Co<sub>4</sub>O<sub>9</sub> improved through ceramic texturing. *J. Mater. Chem.*, 2003, **13**, 1094–1099.
4. Itoh, T. and Terasaki, I., Thermoelectric properties of Bi<sub>2.3-x</sub>Pb<sub>x</sub>Sr<sub>2.6</sub>Co<sub>2</sub>O<sub>y</sub> single crystals. *Jpn. J. Appl. Phys.*, 2000, **39**, 6658–6660.
5. Funahashi, R., Matsubara, I., Ikuda, H. and Takeuchi, T., An oxide single crystal with high thermoelectric performance in air. *Jpn. J. Appl. Phys.*, 2000, **39**, L1127–L1129.
6. Ishiguro, T., Kitazawa, A., Mizutani, N. and Kato, M., Single-crystal growth and crystal structure refinement of CuAlO<sub>2</sub>. *J. Solid State Chem.*, 1981, **40**, 170–174.
7. JCPDS Card File: 35-1401.
8. JCPDS Card File: 02-1040.
9. Shannon, R. D., Rogers, D. B. and Prewitt, C. T., Chemistry of noble metal oxides. I. Syntheses and properties of ABO<sub>2</sub> delafossite compounds. *Inorg. Chem.*, 1971, **10**, 713–718.
10. Kingery, W. D., Bowen, H. K. and Uhlmann, D. R., *Introduction to Ceramics (2nd ed.)*. John Wiley & Sons, New York, 1976, p. 519.
11. Kofstad, P., *Nonstoichiometry, Diffusion, and Electrical Conductivity in Binary Metal Oxides*. Wiley-Interscience, New York, 1972, p. 19.
12. Benko, F. A. and Koffyberg, F. P., Opto-electronic properties of CuAlO<sub>2</sub>. *J. Phys. Chem. Solids*, 1984, **45**, 57–59.
13. Kawazoe, H., Yasukawa, M., Hyodo, H., Kurita, M., Yanagi, H. and Hosono, H., P-type electrical conduction in transparent thin films of CuAlO<sub>2</sub>. *Nature*, 1977, **389**, 939–942.
14. Banerjee, A. N., Maity, R. and Chattopadhyay, K. K., Preparation of p-type transparent conducting CuAlO<sub>2</sub> thin films by reactive DC sputtering. *Mater. Lett.*, 2003, **58**, 10–13.
15. Yanagi, H., Inoue, S.-I., Ueda, K., Kawazoe, H. and Hamada, N., Electronic structure and optoelectronic properties of transparent p-type conducting CuAlO<sub>2</sub>. *J. Appl. Phys.*, 2000, **88**, 4159–4163.
16. Uemura, K. and Nishida, I., *Thermoelectric Semiconductors and their Application*. Nikkan-Kogyo Shinbun Press, Tokyo, Japan, 1988.
17. Moon, J.-W., Seo, W.-S., Okabe, H., Okawa, T. and Koumoto, K., Ca-doped RCoO<sub>3</sub> (R=Gd, Sm, Nd, Pr) as thermoelectric materials. *J. Mater. Chem.*, 2000, **10**, 2007–2009.